AD-A120 257 ARMY MATERIALS AND MECHANICS RESEARCH CENTER WATERTOWN MA F/G 11/4
STUDIES OF TENSION TEST SPECIMENS FOR COMPOSITE MATERIAL TESTIN--ETC(U)
APR 82 D W OPLINGER, K R GANDHI, B S PARKER
UNCLASSIFIED AMMRC-TR-82-27 NL

END
DATE FILMED
11 82
DTIC

(12)

AMMRC TR 82-27

STUDIES OF TENSION TEST SPECIMENS FOR COMPOSITE MATERIAL TESTING

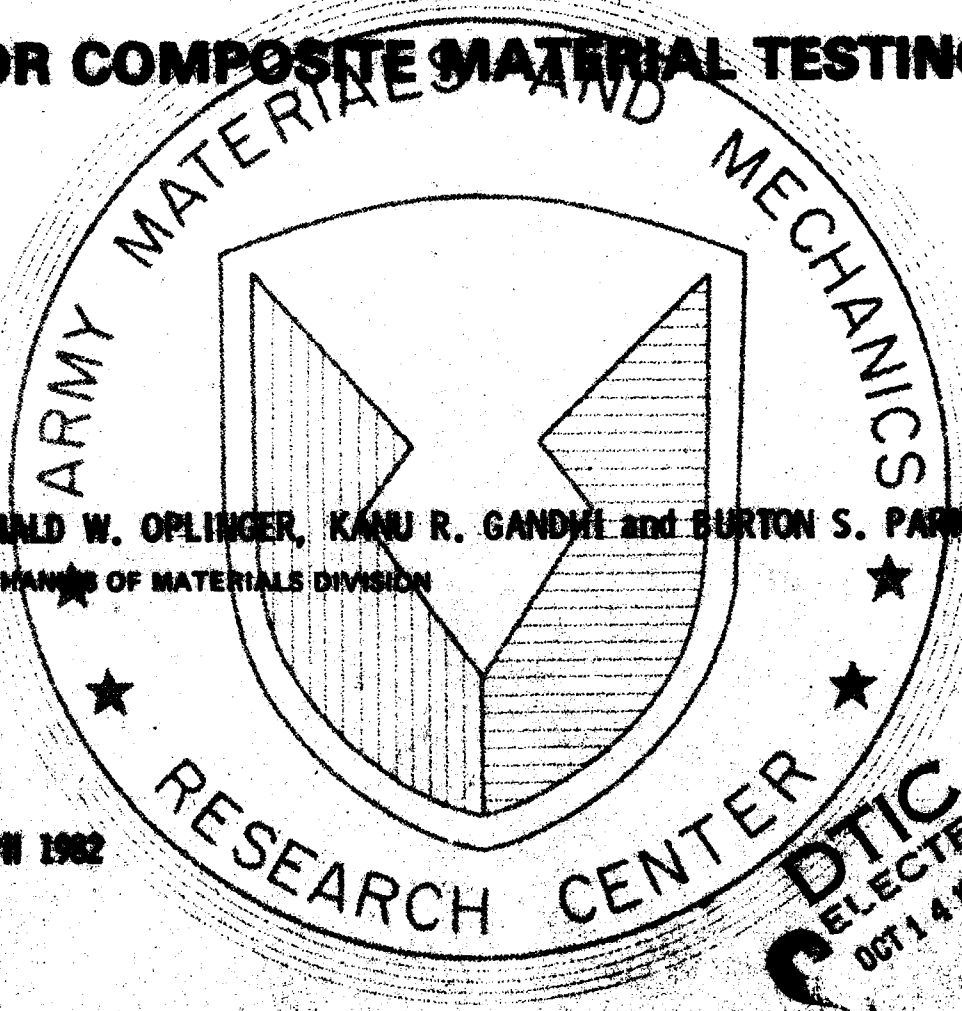

DONALD W. OPLINGER, KANU R. GANDHI and BURTON S. PARKER
MECHANICS OF MATERIALS DIVISION

April 1982

Approved for public release; distribution unlimited.

ARMY MATERIALS AND MECHANICS RESEARCH CENTER
Watertown, Massachusetts 02172

The findings in this report are not to be construed as an official Department of the Army position, unless so designated by other authorized documents.

Mention of any trade names or manufacturers in this report shall not be construed as advertising nor as an official indorsement or approval of such products or companies by the United States Government.

[redacted]

UNCLASSIFIED

SECURITY CLASSIFICATION OF THIS PAGE (When Data Entered)

REPORT DOCUMENTATION PAGE	READ INSTRUCTIONS BEFORE COMPLETING FORM
1. REPORT NUMBER: AMMRC TR-82-27	2. GOVT ACCESSION NO.: AD-A120257
	3. RECIPIENT'S CATALOG NUMBER:
4. TITLE (and Subtitle): STUDIES OF TENSION TEST SPECIMENS FOR COMPOSITE MATERIAL	5. TYPE OF REPORT & PERIOD COVERED: Final Report
	6. PERFORMING ORG. REPORT NUMBER:
7. AUTHOR(s): Donald W. Oplinger, Kanu R. Gandhi and Burton S. Parker	8. CONTRACT OR GRANT NUMBER(s):
9. PERFORMING ORGANIZATION NAME AND ADDRESS: Army Materials and Mechanics Research Center, Watertown, Massachusetts 02172, DRXMR-SM	10. PROGRAM ELEMENT, PROJECT, TASK AREA & WORK UNIT NUMBERS: D/A Project: 1L162105AH84
11. CONTROLLING OFFICE NAME AND ADDRESS: U.S. Army Materiel Development and Readiness Command, Alexandria, Virginia 22333	12. REPORT DATE: April 1982
	13. NUMBER OF PAGES: 21
14. MONITORING AGENCY NAME & ADDRESS(if different from Controlling Office)	15. SECURITY CLASS. (of this report): Unclassified
	15a. DECLASSIFICATION/DOWNGRADING SCHEDULE

16. DISTRIBUTION STATEMENT (of this Report)

Approved for public release; distribution unlimited.

17. DISTRIBUTION STATEMENT (of the abstract entered in Block 20, if different from Report)

18. SUPPLEMENTARY NOTES

Presented at TTCP REVIEW, Technical Panel TP-3 (Organic Materials), Ottawa, 24th Meeting, May, 1978.

19. KEY WORDS (Continue on reverse side if necessary and identify by block number)

Fiber composites
Tensile properties
Tension tests

20. ABSTRACT (Continue on reverse side if necessary and identify by block number)

(SEE REVERSE SIDE)

DD FORM 1 JAN 73 1473 EDITION OF 1 NOV 65 IS OBSOLETE

UNCLASSIFIED

SECURITY CLASSIFICATION OF THIS PAGE (When Data Entered)

Block No. 20

ABSTRACT

This report covers stress analysis and experimental studies of four types of tension specimens designed for testing composite materials. Two ASTM specimen types (D3039 tab-ended and D638 dogbone) are considered, along with the bowtie (flat bar with linear taper) design developed by Grumman and a streamline design developed at AMMRC. Stress analyses of the first three types show them to be subjected to high shear stresses and tensile stress concentrations which tend to degrade their performance. Experimental studies generally tended to confirm that failures initiated where the stress peaks were predicted, and suggest that elimination of such peaks would lead to a better-performing tension specimen. Stress analysis of the AMMRC streamline design showed low shear stress levels and indicated that the design is free of tensile stress concentrations. Results of efforts aimed at experimental evaluation of the streamline specimen indicate that it has much promise as an improved design for tension testing, both under monotonic and cyclic loading.

CONTENTS

	Page
SUMMARY	1
INTRODUCTION	1
SPECIMEN TYPES OF INTEREST	2
ANALYTICAL EFFORTS	
General Remarks	2
Tabbed Specimens	3
D638 Specimens	6
Bowtie Specimens	7
EXPERIMENTAL STUDIES	
Specimen Geometries and Materials	8
Tabbed Specimen Fabrication	9
Types of Study	9
Failure Characteristics	10
Comparison of Tension Test Results	11
Discussion of Experimental Results	15
DEVELOPMENT OF THE STREAMLINE SPECIMEN SHAPE	16
CONCLUSIONS	18

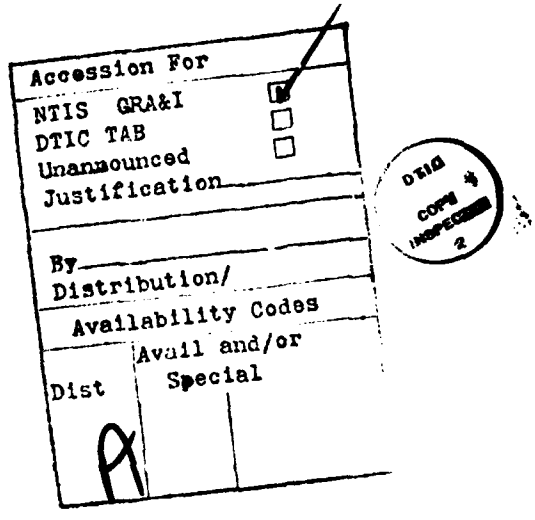

SUMMARY

This report covers stress analysis and experimental studies of four types of tension specimens designed for testing composite materials. Two ASTM specimen types (D3039 tab-ended and D638 dogbone) are considered, along with the bowtie (flat bar with linear taper) design developed by Grumman and a streamline design developed at AMMRC. Stress analyses of the first three types show them to be subjected to high shear stresses and tensile stress concentrations which tend to degrade their performance. Experimental studies generally tended to confirm that failures initiated where the stress peaks were predicted, and suggest that elimination of such peaks would lead to a better-performing tension specimen. Stress analysis of the AMMRC streamline design showed low shear stress levels and indicated that the design is free of tensile stress concentrations. Results of efforts aimed at experimental evaluation of the streamline specimen indicate that it has much promise as an improved design for tension testing, both under monotonic and cyclic loading.

INTRODUCTION

Accepted test specimens used for tension testing of composite materials suffer from such deficiencies as failures not occurring in a uniform-width gage region, which is believed to give low strength values that do not accurately characterize the material under test. In both ASTM specimens shown in Figure 1 typical failures occur away from the uniform-cross-section

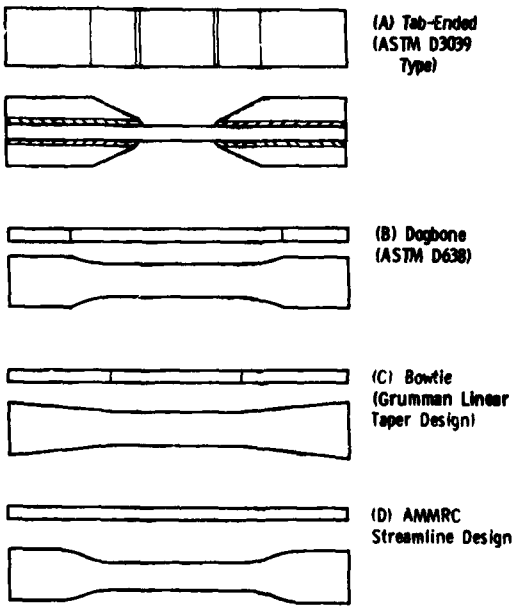

Figure 1. Specimen types under consideration.

region in the center of the specimen. The objective of this study was to develop a specimen design which is free of such behavior and which would lead to test results which more accurately reflect the true strength of the material. The study involved stress analysis of the types of specimen which were of interest, development of a design approach for eliminating stress concentrations which are believed to be the cause of poor specimen performance, and an experimental program having the two-fold objective of (1) verifying the relation between theoretical stress concentrations and observed modes of failure in specimen designs of interest and (2) verifying the performance improvements obtained from designs which are free of stress concentrations.

Although the effort was aimed primarily at specimens for testing of fiberglass-reinforced materials, there is reason to believe that any specimen improvements which can be demonstrated will be applicable not only to composites reinforced with fiberglass, but to composites with other reinforcement types, as well as to bulk polymers which behave brittlely and are therefore sensitive to the presence of stress concentrations.

SPECIMEN TYPES OF INTEREST

Figure 1 shows the types of specimens which have been considered in the study. Figures 1A and 1B show standard ASTM designs which are in widespread use. The "bowtie" design, Figure 1C, a flat bar with a linear taper connecting the grip region with the gage region, was introduced by Grumman (Ref. 1,2) in studies in support of MIL-HDBK-17A (Ref. 3). The "streamline" design of Figure 1D is an AMMRC development resulting from the present study.

ANALYTICAL EFFORTS

General Remarks

Stress analysis studies were performed on each of the specimen designs of Figure 1 using the well-known finite-element method. The main requirement of a good specimen design being the achievement of maximum tensile stresses in the constant width center section or "gage" region, attention in the analytical efforts was directed primarily at uncovering peak tensile stresses outside the gage region which could lead to premature failures during the test. In addition, high shear stresses in the expanding part of the specimen were felt to be objectionable, especially in the flat bar designs of Figure 1B to 1D, since these would cause premature damage in the expanding region

1. DASTIN, S., LUBIN, G., MUNYAK, J., and SLOBODZINSKI, A. *Determination of Principal Properties of E-Fiber-Glass High Temperature Epoxy Laminates for Aircraft.* Final Report, Contract DAAA21-68-C-0404, August 1969
2. DASTIN, S., LUBIN, G., MUNYAK, J., and SLOBODZINSKI, A. *Mechanical Properties and Test Techniques for Reinforced Plastic Laminates.* American Society for Testing and Materials Special Technical Publication STP 460, 1970, p. 13-26.
3. MIL-HDBK-17A, *Plastics for Aerospace Vehicles, Part I* in Reinforced Plastics, January 1971.

of the specimen, thereby defeating its proper function. Thus shear stresses in the expanding region were of interest. In the case of Figure 1B to 1D, maximum shear stresses less than about 10% of the gage-section tensile stresses were felt to be desirable. This corresponds roughly with the ratio of shear-to-tensile strengths of the composite materials which were of interest. In the case of tabbed specimens, Figure 1A, peel stresses (tensile stresses in the lateral direction) in the bond layer between the tab and main specimen body could lead to debonding and were of equal interest with the shear stresses in the bond layer. Discussion of the stress analysis of the design shown in Figure 1D will be postponed to a later section where development of the streamline design concepts is discussed.

Tabbed Specimens

Figure 2 shows the geometry which was considered in the analysis of tabbed specimens. Interest centered on stresses along the line B - B passing through the tab-specimen bondline, with a boundary condition of uniform horizontal motion along line A - A, representing the tab surface in contact with a test machine wedge grip surface, the load being reacted at the right side of the sketch in the form of a uniform nominal tensile stress σ_{nom}. The specimen shown in Figure 2 represents a ±45% E glass epoxy tab (Region 1) bonded to a specimen body (Region 2) of 71.5% 0°/28.5% 90° E glass epoxy material. The tab bevel angle, α, was given values of 10°, 20°, 30° and 90° in the analysis. Tab and specimen thickness values of 0.125" and 0.068" (3.17 mm and 1.73 mm, respectively) were assumed for all cases. Bondline stress distributions which were calculated are shown in Figure 3 as multiples of σ_{nom}, while Figure 4 focuses on the peak values of the three stresses as functions of the tab bevel angle α. Note that the peak stress σ_y and

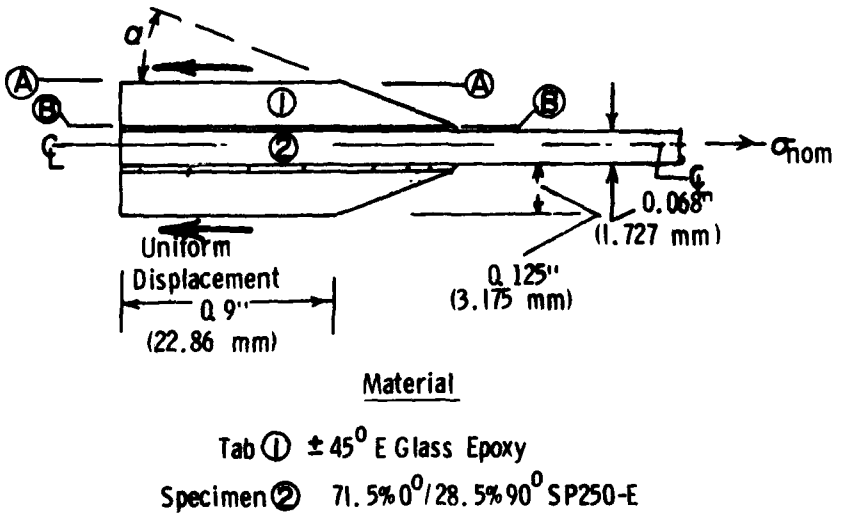

Figure 2. Tab specimen model assumed in stress analysis.

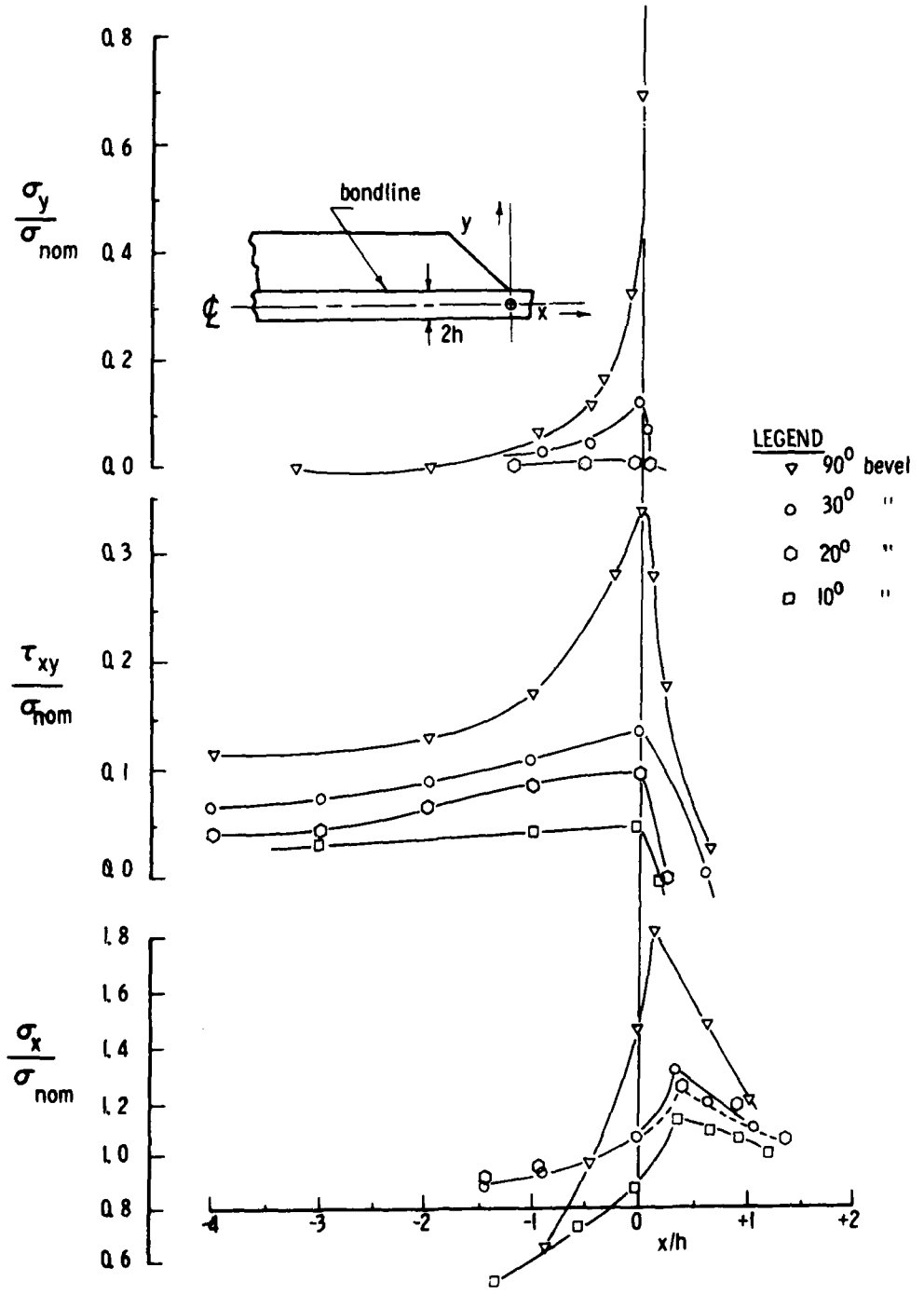

Figure 3. Theoretical stresses in tabbed specimens.

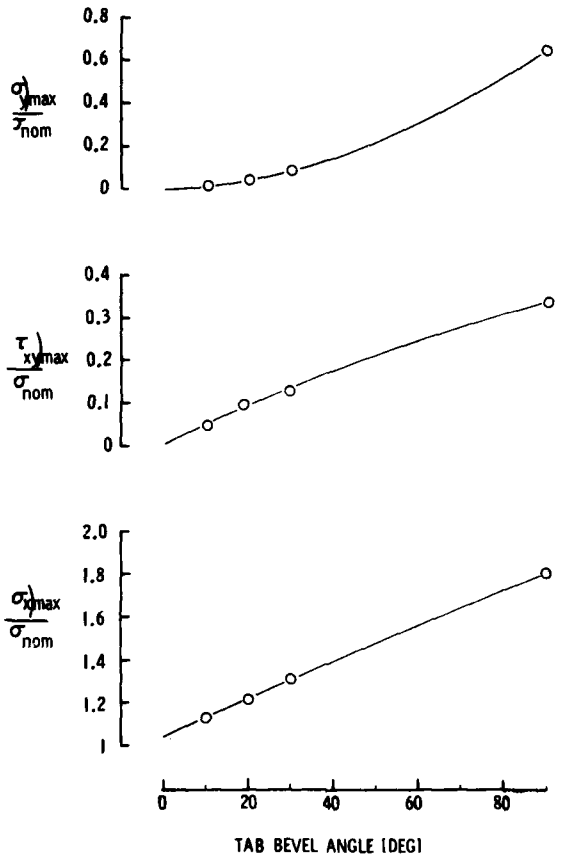

Figure 4. Peak stress versus tab angle.

bond shear stress τ_{xy} relate to the tendency for tabs to debond prior to tensile failure in the specimen, and values of σ_y or τ_{xy} much above about 5% σ_{nom} would be expected to give rise to such debonding for typical specimen materials. The tensile stress concentration, σ_x/σ_{nom}, on the other hand, is associated with the tendency for premature tensile failures to occur in the vicinity of the end of the bevel. Judging from the results in Figure 4, tab angles of 30° or less make the peak stress σ_y small enough to be negligible, while the σ_x and τ_{xy} stress peaks are significant factors even for tab angles as small as 10°. It is useful to note that the latter stresses appear to be nearly linear functions of the bevel angle.

It should be understood that the stress distribution at the very end of the bevel is not accurately predicted by standard finite element methods inasmuch as one generally expects mathematical infinities to occur in the stress distribution when a re-entrant corner formed by the junction of two straight boundaries is present in a solid body. The predicted stress peaks are more in the order of averaged stresses over the mesh element used to model the region near the bevel end. Nonetheless, the trends which are observed as a function of bevel angle are of interest, and there is reason to believe that high predicted stress values occurring with high bevel angles represent a greater tendency toward tab debonding.

Based on these results one can expect tab debonding to be a persistent problem of tabbed specimens even for 10° tabs. Once debonding occurs, the bondline takes on the appearance of a crack under "MODE II" or shear loading. Fracture-mechanics-type concepts need to be applied to the interpretation of stress analyses of such situations, but in any case, it is expected that the peak values of σ_x/σ_{nom} might be considerably more severe for such cases.

D638 Specimens

Figure 5 shows the system which was used to model the ASTM D638 "dogbone" specimen, together with pertinent results from the stress analysis. (The tensile stress in the Y-direction was negligible and is not considered here.) Note that peak τ_{xy} amounting to 14% of σ_{nom} is encountered along the curved part of the boundary at about 0.2" (5.1 mm) away from the end of the horizontal boundary in the grip region. Moreover, a peak tensile stress amounting to 114% of σ_{nom} occurs at about 0.7" (17.8 mm) from the start of the curved boundary along the line y = 0.25" (6.4 mm) representing the extension of the horizontal boundary of the gage region.

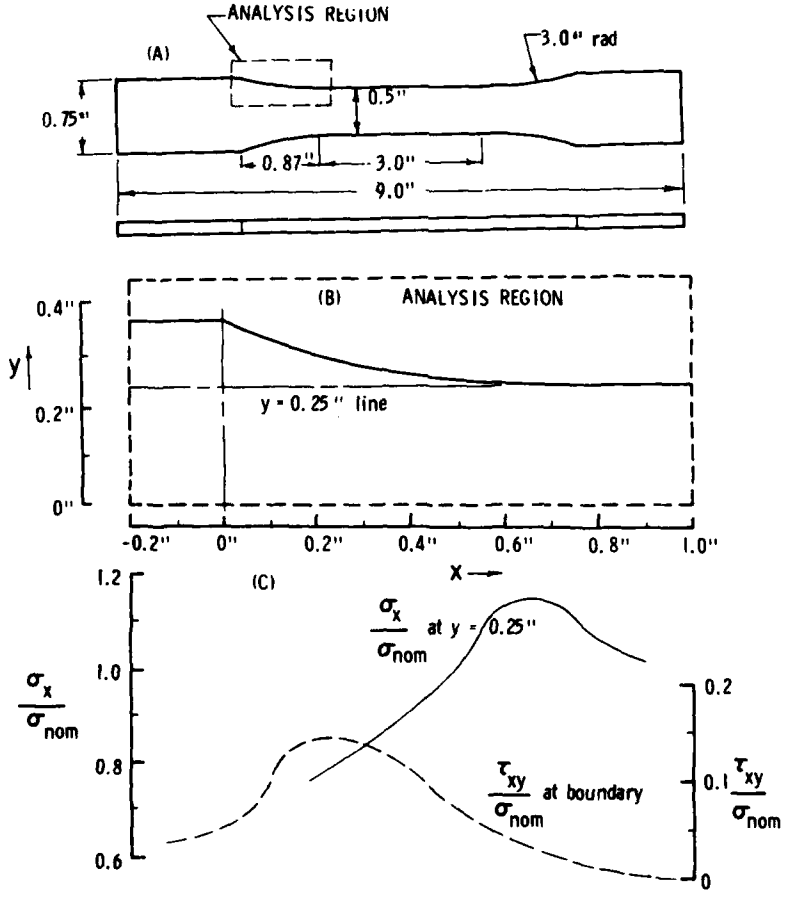

Figure 5. D638 specimen and stresses.

These results indicate that premature shear failure will again occur with this specimen, and that tensile stress concentrations may give rise to non-grip failures at low values of σ_{nom}. Both types of failure are realized in practice as will be discussed subsequently.

Bowtie Specimens

Stress analyses of bowtie specimens were performed for three values of taper angle corresponding to 5%, 10% and 12.5% slopes as shown in Figure 6.

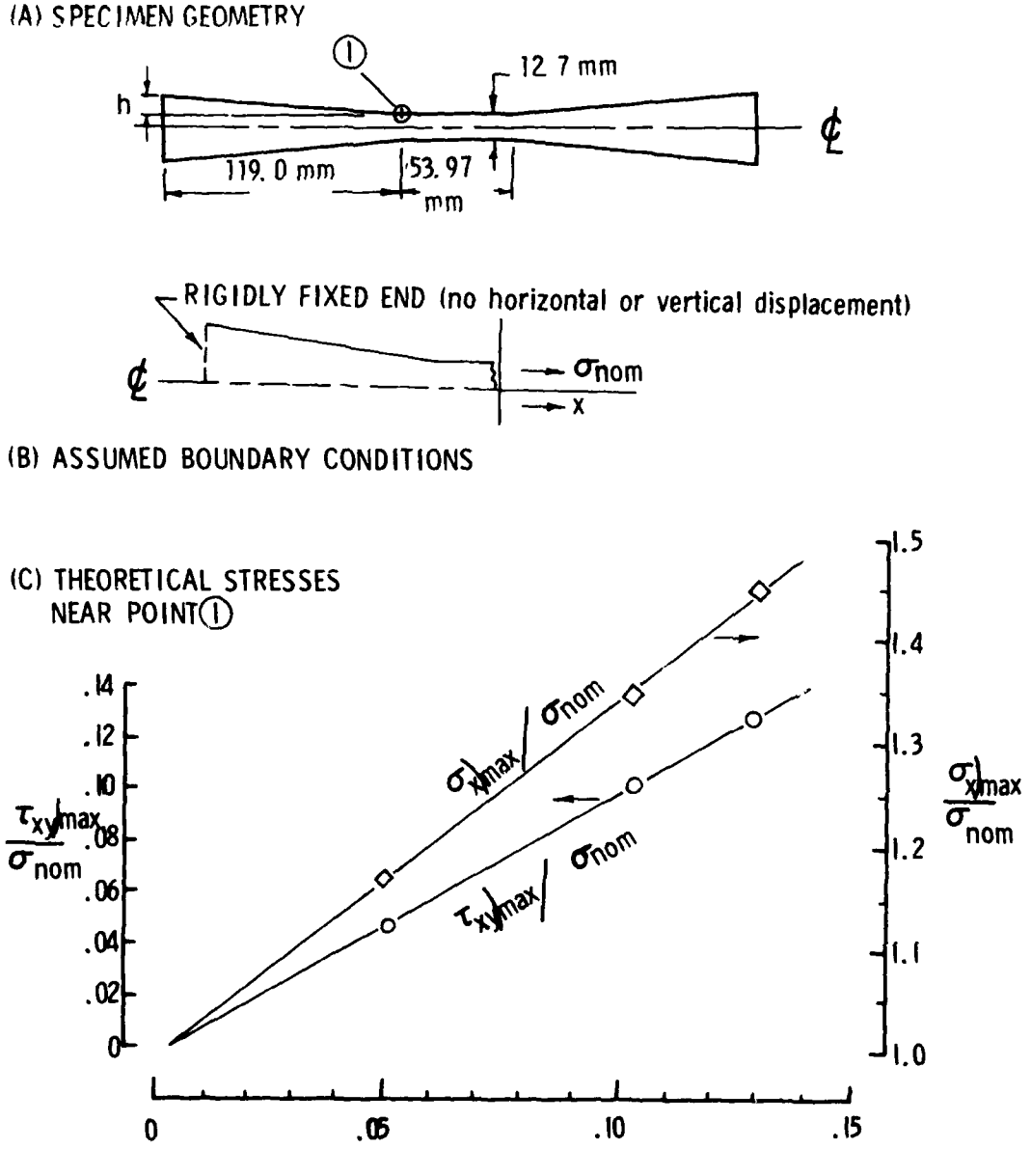

Figure 6. Predicted maximum stresses in bowtie specimen.

Stresses shown in Figure 6C correspond to point 1 identified in Figure 6A at the juncture of the horizontal and inclined segments of the boundary. Again the stress σ_y in the lateral direction was found to be negligible, but significant peaks in the shear and tensile stress distributions were observed near point 1. As indicated in Figure 6C, these are essentially linear functions of the slope of the tapered boundary, given by

$$\tau_{xy}/_{max} \cong S\,\sigma_{nom}$$

$$\sigma_x/_{max} \cong \sigma_{nom}\ (1+3.5\ S)$$

where S is the slope of the taper region, i.e.,

$$S = \frac{h(in)}{4.687} = \frac{h(cm)}{11.9}$$

corresponding to Figure 6A in which 4.687" (11.9 cm) is the horizontal length of the taper, h its height. Specific cases which have been analyzed or considered experimentally give the results shown in Table 1. The first entry in Table 1

Table 1. MAXIMUM STRESSES IN BOWTIE SPECIMENS

Where Reported	Slope	$\frac{\tau_{xy/max}}{\sigma_{nom}}$	$\frac{\sigma_{x/max}}{\sigma_{nom}}$
Grumman, Ref. 1,2	0.0266	0.027	1.09
AMMRC "A"	0.05	0.05	1.175
AMMRC "B"	0.10	0.10	1.35
AMMRC "C"	0.125	0.125	1.46

refers to the original bowtie specimen developed at Grumman (Ref. 1,2) and used for data reported in MIL-HDBK-17A (Ref. 3). The other entries refer to AMMRC specimens which were subjected to both stress analysis and experimental studies. As discussed later, shear failures were observed for specimen slopes of 0.10 and above, and localized tensile failures were experienced for all AMMRC specimens, indicating the level of shear and tensile stress peaks to be objectionable for slopes equal to 0.10 or greater. Favorable results reported by Grumman for the 2.7% slope specimen suggest that the stress peaks for this slope are acceptably low.

EXPERIMENTAL STUDIES

Specimen Geometries and Materials

Experimental studies were carried out on tabbed specimens, D638 specimens and bowtie-type specimens. Geometries for the tabbed and bowtie specimens are shown in Figures 7 and 8, while the geometry shown in Figure 5A was used for D638 specimens. The specimen materials consisted of 14 plies of 3M's SP250E (E glass epoxy) arranged in a 0°(71.5%)/90°(28.5%) stacking sequence (i.e., $0_{10}/90_4$). For the tabbed specimens, tabs were bonded using FM1000 film adhesive.

Tabbed Specimen Fabrication

Tabs were bonded using a special coffin-mold fixture for holding the assembly in place and appplying clamping pressure. There was concern that for low tab angles, poor bonding might occur at the part of the bondline where the tab bevel is located, due to the lack of clamping pressure there. Accordingly, a technique was devised, as shown in Figure 9, whereby an insert having a slope equal to that of the bevel was located to allow for transmission of clamping pressure from the flat surface of the clamping platen to the sloping part of the tab. Other than this feature, standard procedures for bonding of the FM1000 film adhesive were followed.

Types of Study

The experimental effort was two-fold in nature, including (1) detailed observation of damage modes in the D638 and bowtie specimens together with cursory examination of failure characteristics of the tabbed specimen and

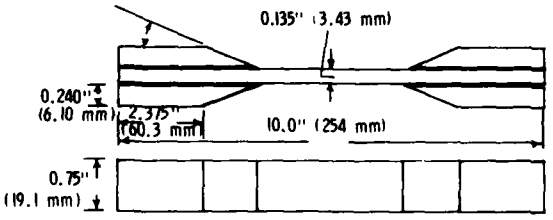

MATERIALS - See Fig. 2

Lot No.	Bevel deg.	Clamping Condition*	No. of Specimens
1	90	U	10
2	30	U	8
3	10	U	3
3C	10	C	7

*C = clamping pressure applied to tab bevel during tab bonding, per Fig. 9
U = bevel unclamped during tab bonding

Figure 7. Tabbed specimens tested.

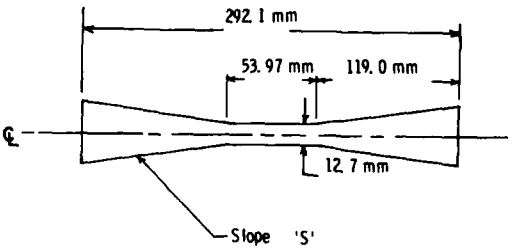

CONFIGURATION	SLOPE 'S'	H in	H mm
A	0.05	0.484	12.29
B	0.100	0.719	18.26
C	0.125	0.836	21.23

Figure 8. Bowtie specimen configurations.

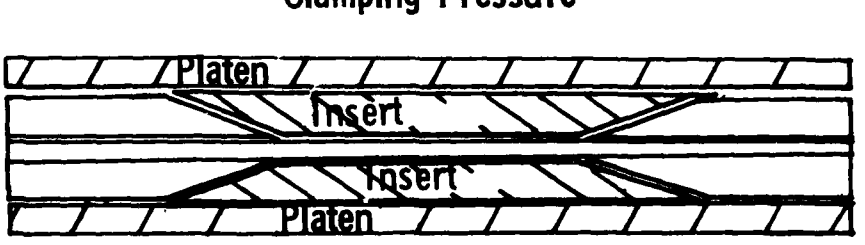

Figure 9. Special arrangement for clamping bevel during tab bonding.

(2) comparison of failure levels measured in the specimen types of interest. Subsequent discussion in this section is arranged in terms of these two aspects of the experimental effort.

Failure Characteristics

General Observation: No gage failures were observed in any of the tests. Invariably specimens broke into strips on the order of 0.25" (6.4 mm) wide which ran the length of the specimen lying between the test machine grips. Initial damage characteristics of the various types of specimens are illustrated in Figure 10.

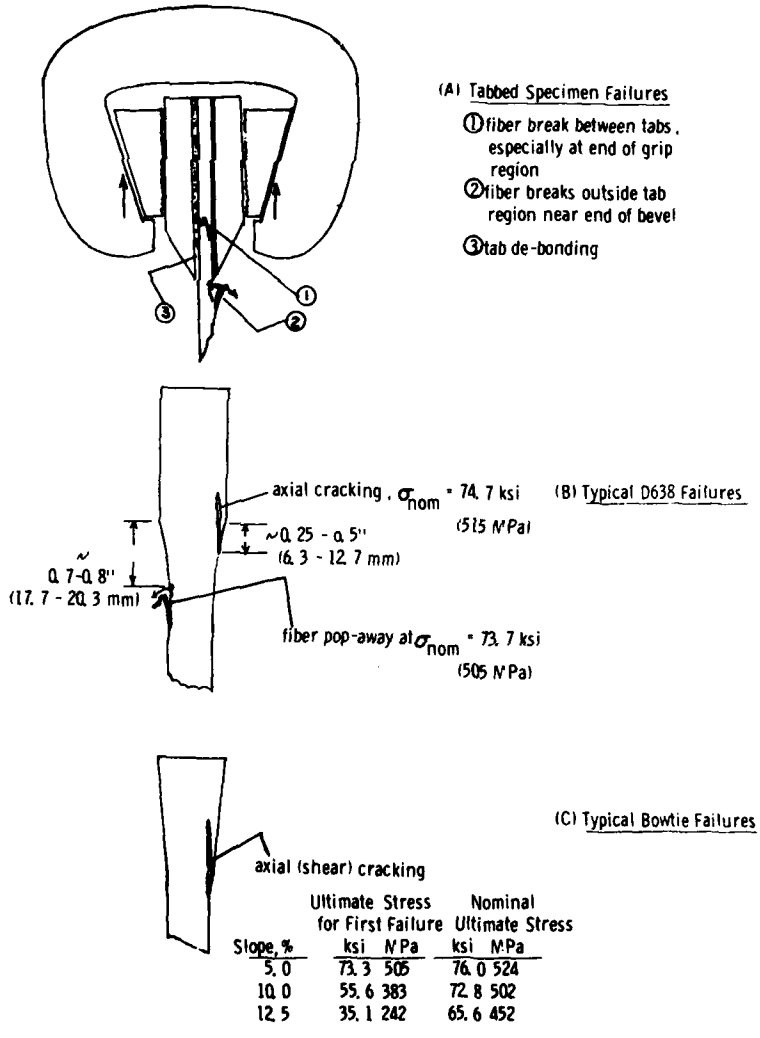

Slope, %	Ultimate Stress for First Failure ksi	MPa	Nominal Ultimate Stress ksi	MPa
5.0	73.3	505	76.0	524
10.0	55.6	383	72.8	502
12.5	35.1	242	65.6	452

Figure 10. Failure characteristics of tension specimens.

Army Materials and Mechanics Research Center
Watertown, Massachusetts 02172
STUDIES OF TENSION TEST SPECIMENS
FOR COMPOSITE MATERIAL -
Donald W. Oplinger, Kanu R. Gandhi
and Burton S. Parker

Technical Report AMMRC TR 82-27, April 1982, 21 pp - illus-tables, D/A Project 1L162105AH84

AD ________________

UNCLASSIFIED
UNLIMITED DISTRIBUTION

Key Words

Fiber composites
Tensile properties
Tension tests

This report covers stress analysis and experimental studies of four types of tension specimen designed for testing of composite materials. Two ASTM specimen types (D3039 tab-ended types and D638 dogbone types) are considered, along with the bowtie (flat bar with linear taper) design developed by Grumman and a streamline design developed at AMMRC. Stress analysis of the first three types show them to be subjected to high shear stresses and tensile stress concentrations which tend to degrade their performance. Experimental studies generally tended to confirm that failures initiated where the stress peaks were predicted, and suggest that elimination of such peaks would lead to a better-performing tension specimen. Stress analysis of the AMMRC streamline design showed low shear stress levels and indicated that the design is free of tensile stress concentrations. Results of efforts aimed at experimental evaluation of the streamline specimen indicate that it has much promise as an improved design for tension testing, both under monotonic and cyclic loading.

Army Materials and Mechanics Research Center
Watertown, Massachusetts 02172
STUDIES OF TENSION TEST SPECIMENS
FOR COMPOSITE MATERIAL -
Donald W. Oplinger, Kanu R. Gandhi
and Burton S. Parker

Technical Report AMMRC TR 82-27, April 1982, 21 pp - illus-tables, D/A Project 1L162105AH84

AD ________________

UNCLASSIFIED
UNLIMITED DISTRIBUTION

Key Words

Fiber composites
Tensile properties
Tension tests

This report covers stress analysis and experimental studies of four types of tension specimen designed for testing of composite materials. Two ASTM specimen types (D3039 tab-ended types and D638 dogbone types) are considered, along with the bowtie (flat bar with linear taper) design developed by Grumman and a streamline design developed at AMMRC. Stress analysis of the first three types show them to be subjected to high shear stresses and tensile stress concentrations which tend to degrade their performance. Experimental studies generally tended to confirm that failures initiated where the stress peaks were predicted, and suggest that elimination of such peaks would lead to a better-performing tension specimen. Stress analysis of the AMMRC streamline design showed low shear stress levels and indicated that the design is free of tensile stress concentrations. Results of efforts aimed at experimental evaluation of the streamline specimen indicate that it has much promise as an improved design for tension testing, both under monotonic and cyclic loading.

Army Materials and Mechanics Research Center
Watertown, Massachusetts 02172
STUDIES OF TENSION TEST SPECIMENS
FOR COMPOSITE MATERIAL -
Donald W. Oplinger, Kanu R. Gandhi
and Burton S. Parker

Technical Report AMMRC TR 82-27, April 1982, 21 pp - illus-tables, D/A Project 1L162105AH84

AD ________________

UNCLASSIFIED
UNLIMITED DISTRIBUTION

Key Words

Fiber composites
Tensile properties
Tension tests

This report covers stress analysis and experimental studies of four types of tension specimen designed for testing of composite materials. Two ASTM specimen types (D3039 tab-ended types and D638 dogbone types) are considered, along with the bowtie (flat bar with linear taper) design developed by Grumman and a streamline design developed at AMMRC. Stress analysis of the first three types show them to be subjected to high shear stresses and tensile stress concentrations which tend to degrade their performance. Experimental studies generally tended to confirm that failures initiated where the stress peaks were predicted, and suggest that elimination of such peaks would lead to a better-performing tension specimen. Stress analysis of the AMMRC streamline design showed low shear stress levels and indicated that the design is free of tensile stress concentrations. Results of efforts aimed at experimental evaluation of the streamline specimen indicate that it has much promise as an improved design for tension testing, both under monotonic and cyclic loading.

Army Materials and Mechanics Research Center
Watertown, Massachusetts 02172
STUDIES OF TENSION TEST SPECIMENS
FOR COMPOSITE MATERIAL -
Donald W. Oplinger, Kanu R. Gandhi
and Burton S. Parker

Technical Report AMMRC TR 82-27, April 1982, 21 pp - illus-tables, D/A Project 1L162105AH84

AD ________________

UNCLASSIFIED
UNLIMITED DISTRIBUTION

Key Words

Fiber composites
Tensile properties
Tension tests

This report covers stress analysis and experimental studies of four types of tension specimen designed for testing of composite materials. Two ASTM specimen types (D3039 tab-ended types and D638 dogbone types) are considered, along with the bowtie (flat bar with linear taper) design developed by Grumman and a streamline design developed at AMMRC. Stress analysis of the first three types show them to be subjected to high shear stresses and tensile stress concentrations which tend to degrade their performance. Experimental studies generally tended to confirm that failures initiated where the stress peaks were predicted, and suggest that elimination of such peaks would lead to a better-performing tension specimen. Stress analysis of the AMMRC streamline design showed low shear stress levels and indicated that the design is free of tensile stress concentrations. Results of efforts aimed at experimental evaluation of the streamline specimen indicate that it has much promise as an improved design for tension testing, both under monotonic and cyclic loading.

Tabbed Specimens: As shown in Figure 10A, failure of tabbed specimens occurred either in the region between the tabs or outside the tab region but close to the end of the bevel. In a few cases tab debonding was apparent. Fiber breaks inside the tab region were often located near the end of the portion subjected to clamping pressure by the test machine grips.

In the case of 10° tabs, the development of shear cracks parallel to and near the bondline were observed in the course of the test in cases where the clamping arrangement of Figure 9 had not been applied during tab bonding. As seen later, low failure levels occurred in these cases.

D638 Specimens: Figure 10B illustrates typical failure characteristics of D638 specimens. Axial cracking occurring at 0.25" to 0.5" (6.4 to 12.7 mm) from the end of the wide portion of the specimen appears to be associated with high shear stresses in this region indicated in Figure 5C, while fiber breaks occurring at about 0.7" to 0.8" (17.8 to 20.3 mm) from the end of the wide portion appear to be associated with the tensile stress peaks shown in Figure 5C. The apparent shear-type failure is also seen in the moiré fringe pattern shown in Figure 11. These fringes represent contours of equal axial displacement, each fringe representing an increment of 0.001" in displacement (0.0254 mm). The spacing of fringes gives a measure of axial tensile strain while curving of the fringes indicates the presence of shear strain. (The pattern at zero load represents a fictitious mismatch strain of about 0.0035 which must be subtracted out of strain measurements at non-zero load). The nature of the pattern at the two highest loads, especially the curving of fringes to the right of the crack, suggests that the material outside the crack continues to be stressed after cracking, and therefore that the crack does not completely penetrate the specimen.

Bowtie Specimen: As illustrated in Figure 10C, initial failures in the bowtie specimens were axial cracks initiating at the end of the tapered region. Typical results for each taper value are shown in Figure 10C in the form of nominal stress for first damage compared with ultimate nominal stress developed by the specimen. Some tendency for fiber breakage to develop at the end of the tapered region was apparent in post-test examination of the bowtie specimens. The nominal stress for first failure decreased with increasing taper angle, consistent with the prediction of higher shear stress with increased taper (Figure 6). Combining the theoretical shear stress predictions with the nominal stresses at which axial cracks occurred does not give a very consistent shear strength value from observations of nominal stresses at which the axial cracks developed, either for the bowtie or D638 specimens. The trend of the bowtie specimens toward lower nominal stress for first damage with higher predicted shear stress is felt to indicate that the shear stresses do have an important controlling effect on development of early damage in the specimen.

Comparison of Tension Test Results

Tension test results for the specimens of interest are given in Figure 12. Generally speaking, the 10° tabbed specimens with the bevel region clamped during tab application give the highest average test results. Results for 30° tabbed, 10° tabbed/unclamped (during bonding) D638 and 5% taper bowtie

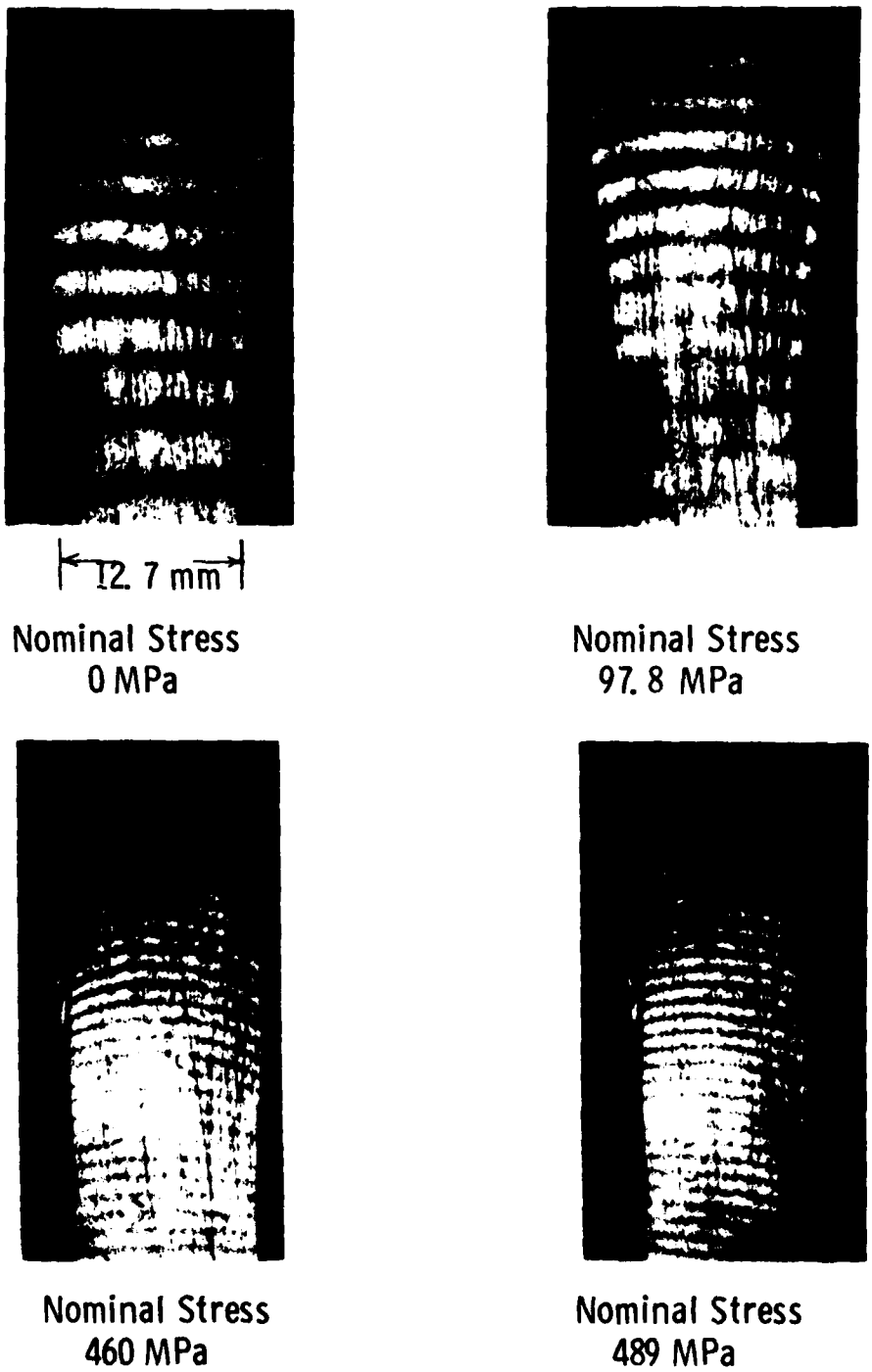

Figure 11. Moire patterns for axial displacement, D638 specimen. 0/90 SP250E glass epoxy. (Grating Density 39.37 l/mm)

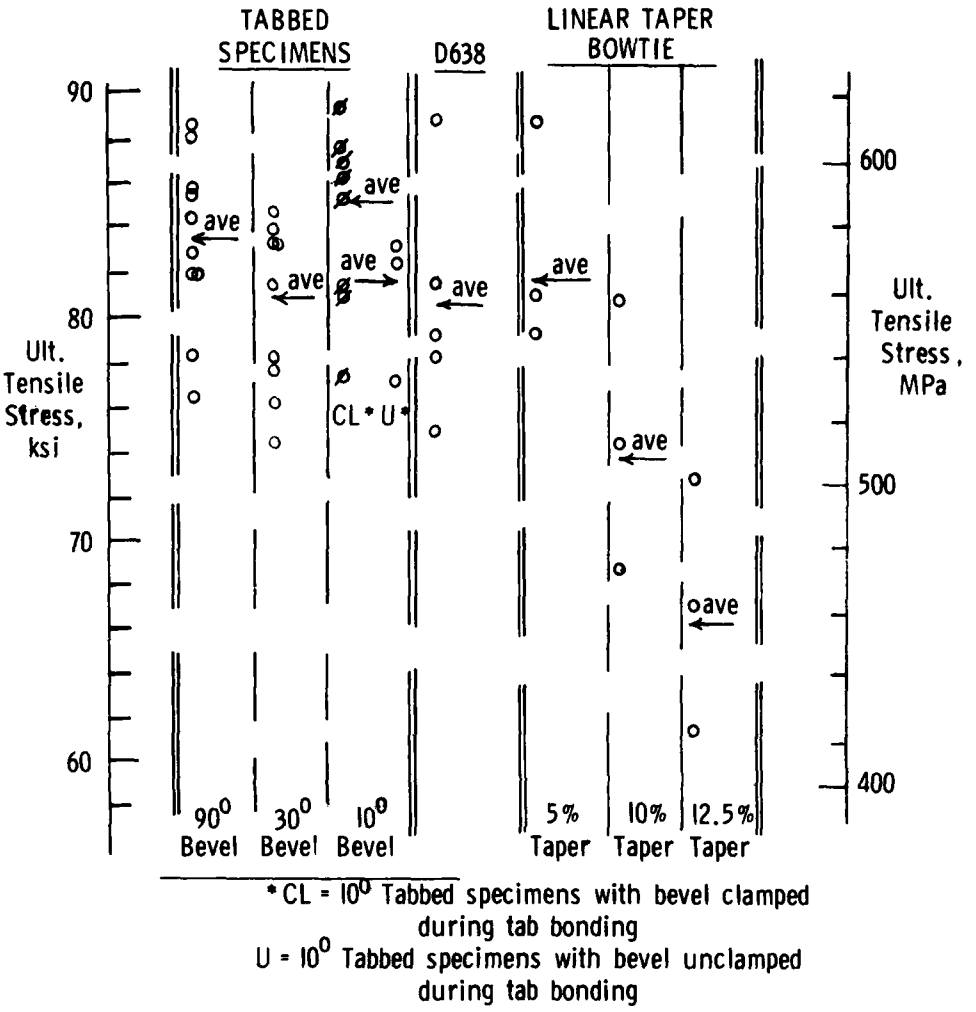

Figure 12. AMMRC test results on SP250E glass epoxy laminates, $0_{10}/90_4$ layup.

gave average test results which were close to identical. The 90° tabbed specimens gave a relatively high average strength; average, highest and lowest values for 90° tabbed specimens were all greater than those of the 30° tabbed specimens, for example, and only slightly less than those of the 10°/clamp-bonded specimens.

During tests of the 10°/unclamped specimens there was a tendency, in those which were closely watched during loading, for shear cracks to develop in the bevel area. With the 10°/clamp-bonded tabs in which shear cracking was absent, the highest of all test results were obtained. However, in a few cases shear cracks were observed in the 10°/clamp-bonded tabs, and in these, low strength values occurred. The statistics of the situation being somewhat sparse, it is apparent that more testing is needed to firmly establish such trends, but there is enough evidence to suggest that such further testing is definitely warranted.

While the 5%-taper bowtie specimens gave results which were comparable to those of other specimens, the 10% and 12.5% tapered specimens fell considerably below. This indicates that exploring the region below 5% taper may give further improvement in the performance of the bowtie specimen. The Grumman results shown in Figure 13 (Ref. 2) for 7781 woven E-glass-reinforced laminates throws more light on the situation. Here the 2.7% taper bowtie configuration gives results which are somewhat above the D638 test results and considerably above those of the 30° tabbed specimens. Furthermore, it was reported in Ref. 2 that failures in the 2.7% taper bowtie specimens were consistently in the gage region, a desirable characteristic of good specimen design. The Grumman results indicate that the low-taper bowtie specimen shows definite promise as an improved specimen design and that the 30° tabbed specimen is inferior to the D638.

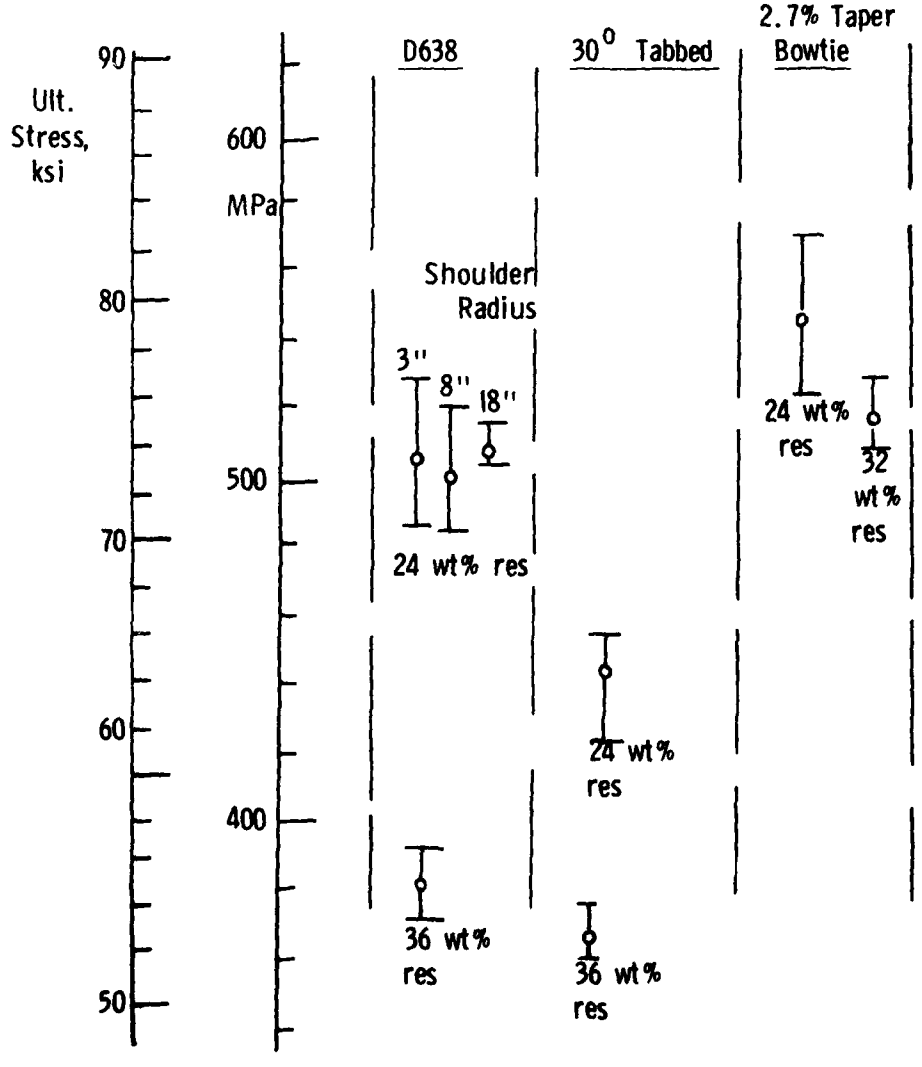

Figure 13. Grumman test results for 7781 woven E - glass/epoxy laminates (Ref. 2) - warp direction.

Discussion of Experimental Results

The primary aim of the experimental studies was to determine to what extent stress concentrations in the specimen can be correlated with initial damage and failure level of each specimen design, and to establish whether reduction of stress concentrations gives improved performance. The data given in Table 2 suggests that the test results for flat-bar type specimens,

Table 2. EXTRAPOLATED LAMINATE STRENGTH VALUES

Extrapolated Strength = Measured Tensile Strength x SCF					
	Measured Strength		Tensile	Extrapolated Strength	
Specimen	ksi	MPa	SCF	ksi	MPa
D638	80.5	555	1.14	91.8	633
Bowtie-5%	81.5	562	1.17	95.3	657
10%	74.0	510	1.34	99.2	684
12%	66.5	459	1.39	92.4	637

i.e., D638 and the three bowtie designs, are reasonably well correlated with tensile stress concentration factors (SCF) taken from Figures 5 and 6 for these specimens; the "extrapolated laminate strength" is simply the maximum laminate tensile stress occurring in the specimen at failure calculated by multiplying σ_{nom} by the SCF. The effective laminate strength obtained by this method lies in the range of 92 to 99 ksi (635 to 683 MPa) which is fairly good agreement considering the scatter of the material. The shear stress for first damage of the axial cracking type is similarly compared for selected individual tests of the flat specimens in Table 3. The bowtie shear failure levels are reasonably close to each other, although the shear stress for first damage of the D638 specimen is higher and considerably out-of-line with the bowtie results.

Table 3. MAXIMUM SHEAR STRESS AT LOAD CAUSING FIRST DAMAGE

		Nominal Stress For First Damage		Maximum Shear Stress At First Damage	
Specimen	Shear SCF	ksi	MPa	ksi	MPa
D638	0.141	60.0	413	8.46	58.2
Bowtie-5%	0.05	73.3	505	3.66	25.2
10%	0.10	55.6	383	5.56	38.3
12.5	0.125	35.1	242	4.39	30.2

In general, it appears that specimen performance correlates well with stress concentration factors predicted by two-dimensional elasticity analysis for the flat-bar specimens.

The same type of evaluation has not been pursued with the tabbed specimens in view of a more complicated failure progression that occurs with tabs, i.e., once tab debonding shear cracking occurs in the tab region, the stresses are likely to undergo considerable readjustment, making initial SCF calculations invalid. As mentioned previously, fracture mechanics analytical approaches are required to evaluate tab specimen performance

if a shear crack or debond is present in the tab area. Results with the 10° clamp-bonded tabs suggest that elimination of initial tab-region cracking by a further decrease of the tab bevel angle in combination with the clamp bonding approach would give a data base for using the predicted SCF values more effectively. Although such research investigations of tab angles less than 10° would be fruitful, the question of practicality of providing specimens with tab bevels less than 10° must be addressed in terms of economy of specimen manufacture. Broadly speaking, the results of the present study suggest that of the tabbed specimens considered, the 90° tabs provide the best compromise of manufacturing economy and performance, the 30° tabs giving the least satisfactory performance. Although 30° bonded tabs are almost an industry standard in the field of advanced composites, they appear to be a poor choice for testing of fiberglass-reinforced materials. Low performance of 30°-tab specimens is especially evident in the results of Ref. 2 cited in Figure 13.

DEVELOPMENT OF THE STREAMLINE SPECIMEN SHAPE

The streamline specimen design is in the tradition of the use of analogies between hydraulic flow and elastic stress fields in bodies of comparable shape which have been described from time to time in the literature (Refs. 4, 5) as a means of designing machine parts having low stress concentration factors. In the present case, the specimen shape is derived from one of the flow lines for the system shown in Figure 14, which represents

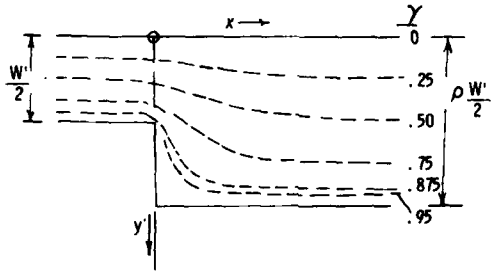

Figure 14. Two-dimensional flow lines in channel with right-angle expansion.

two-dimensional flow in a channel with an abrupt right-angled expansion. The solution of the flow field, i.e., the shapes of the flow lines, can be calculated in closed form by well-known methods (Ref. 6) involving the application of the Schwarz-Christoffel transformation in conjunction with an analytic function representation of the problem. The analogy which is used to relate the stress field in the tension specimen to the flow field in Figure 14 requires a scale change for the y-coordinate given by

$$y = y'\sqrt{E_x/G_{xy}} \ ,$$

4. PETERSON, R. E. *Stress Concentration Factors.* John Wiley & Sons, Inc., New York, 1974, p. 83-84.
5. HEYWOOD, B. *Designing by Photoelasticity.* Chapman and Hall, Ltd., London, 1st ed, 1952.
6. WALKER, M. *The Schwartz-Christoffel Transformation and Its Application - A Simple Exposition.* Dover Publications, New York, 1964, p. 53-65.

where y' is the lateral coordinate in the flow field problem of Figure 14, y the related coordinate in the elastic stress field, and E_x and G_{xy} are axial Young's modulus and shear modulus of the material being tested. The parameter γ in Figure 14 represents the dimensionless position in the y' direction of the flow line under consideration at the far right end of the system where the lines are parallel; i.e., $\gamma = 0.5$ refers to a flow line which is halfway between the straight upper boundary and the lower boundary containing the change in shape, $\gamma = 0.25$ refers to the line lying 1/4 the distance from the upper to the lower boundary, etc.

Studies have shown that tension specimens having boundary shapes corresponding to flow lines for which γ is not greater than 0.5 successfully eliminate intermediate tensile stress peaks in the expanding part of the specimen. In addition, for γ less than about 0.4, the shear stress can be limited to about 6% of σ_{nom}, an acceptable level. Figure 15, for example,

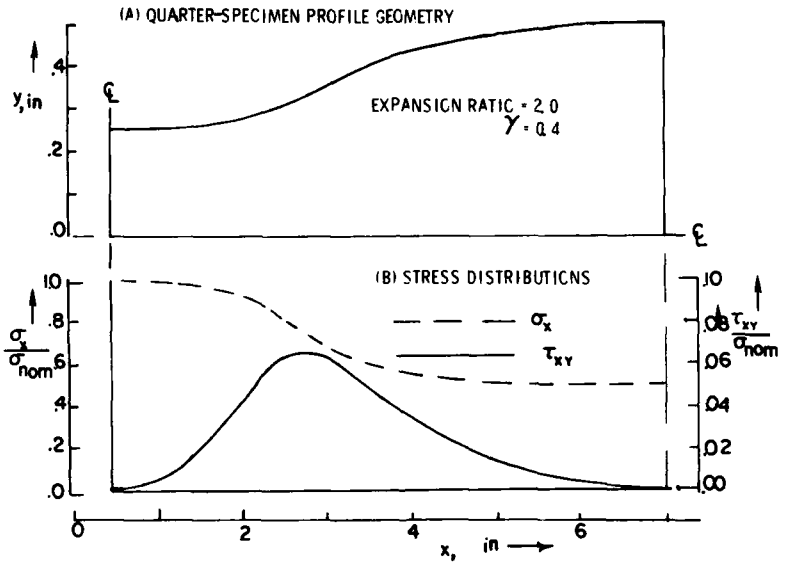

Figure 15. Stresses in typical streamline specimen.

shows the distribution of σ_x and τ_{xy} along the boundary (where these are maximum for a given x) of a specimen for which $\gamma = 0.4$. Figure 15A shows the geometry for one quarter of the specimen, while Figure 15B shows the predicted stresses. It is clear that σ_x is nowhere higher than in the gage region where it reaches a value of 1.0, the value of σ_{nom}. Peak shear stresses of about 0.065 or 6.5% of σ_{nom} appear to be quite acceptable. Figure 16 shows the half-specimen geometry based on the profile of Figure 15.

Several experimental programs aimed at evaluation of the streamline specimen have been underway at AMMRC for glass epoxies and graphite epoxies, as well as for non-fibrous materials such as structural foams and homogeneous plastics. These efforts have been conducted under both monotonic and cyclic loading. Results of these efforts, which will be reported subsequently, indicate that the streamline specimen design has much promise an an improved specimen for tension testing. In addition to in-house evaluation, a program of round-robin testing of graphite epoxies, aimed at a comparison of the streamline shape with the D3039 tabbed specimen, has been supported by AMMRC in conjunction with ASTM Committee D30.04.

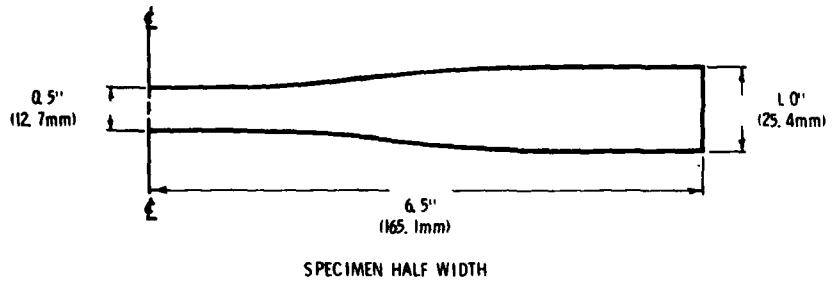

Figure 16. Half-specimen geometry for specimen of Figure 15.

CONCLUSIONS

Results of the present study give strong evidence that poor performance of tension test specimens for glass-reinforced composites is associated with the presence of tensile stress concentrations in the test specimen, and that elimination of such stress concentrations by improved design of the specimen geometry will result in desirable improvements of tensile strength measurements.

The streamline specimen shape is capable of complete elimination of tensile stress concentrations, with marked freedom from shear stresses which can cause first damage to occur at low nominal stress values.

Bowtie specimens having taper ratios less than 5% look promising, especially in view of the results reported in Ref. 2.

Flat specimens with well-designed transition regions appear to be generally more desirable than tabbed specimens. Not only do they promise better ultimate performance, but the manufacturing economy seems favorable in view of the possibility of mass producing flat specimens by template-controlled routers. AMMRC is currently undergoing an assessment of specimen machining methods in which numerical control methods will be compared with template-controlled profiles, etc.

In the case of tabbed specimens, 90° tabs appear to give adequate performance at minimum fabrication effort. Bevelled tabs of greater than 10° bevel angles appear to be inferior, especially if measures are not taken to clamp the bevel during tab application.

DISTRIBUTION LIST

No. of Copies	To
1	Office of the Under Secretary of Defense for Research and Engineering, The Pentagon, Washington, DC 20301
12	Commander, Defense Technical Information Center, Cameron Station, Building 5, 5010 Duke Street, Alexandria, VA 22314
	Metals and Ceramics Information Center, Battelle Columbus Laboratories, 505 King Avenue, Columbus, OH 43201
1	ATTN: Mr. Robert J. Fiorentino, Program Manager
1	Mr. Harold Mindlin, Director
	Defense Advanced Research Projects Agency, Defense Sciences Office/MSD, 1400 Wilson Boulevard, Arlington, VA 22209
1	ATTN: LTC Loren A. Jacobson
	Headquarters, Department of the Army, Washington, DC 20314
1	ATTN: DAEN-RDM, Mr. J. J. Healy
	Deputy Chief of Staff for Research, Development, and Acquisition, Headquarters, Department of the Army, Washington, DC 20310
1	ATTN: DAMA-ARZ
1	DAMA-ARZ-E
1	DAMA-CSS
	Commander, Army Research Office, P.O. Box 12211, Research Triangle Park, NC 27709
1	ATTN: Information Processing Office
1	Dr. F. Schmiedeshoff
1	Dr. G. Mayer
1	Mr. J. J. Murray
	Commander, U.S. Army Materiel Development and Readiness Command, 5001 Eisenhower Avenue, Alexandria, VA 22333
1	ATTN: DRCQA-E
1	DRCQA-P
1	DRCDMD-FT
1	DRCMT
1	DRCMM-M
	Commander, U.S. Army Foreign Science and Technology Center, 220 7thStreet, N.E., Charlottesville, VA 22901
1	ATTN: DRXST-SD3, Military Tech, Mr. Marley
	Commander, U.S. Army Engineer School, Fort Belvoir, VA 22060
1	ATTN: Library
	Commander, U.S. Army Engineer Waterways Experiment Station, Vicksburg, MS 39180
1	ATTN: Research Center Library
	Commander, U.S. Army Materiel Systems Analysis Activity, Aberdeen Proving Ground, MD 21005
1	ATTN: DRXSY-MP, H. Cohen
	Commander, U.S. Army Research and Engineering Directorate, Warren, MI 48090
1	ATTN: SMOTA-RCM.1, Mr. Edward Moritz
	Director, U.S. Army Air Mobility Research and Development Laboratory, Advanced Technology Center, Fort Eustis, VA 23604
1	ATTN: DAVDL-ATL-ATS, J. Waller
1	DAVDL-ATL-ATP, J. Gomes
1	DAVDL-ATL-ASV, Safety and Surv Tech Area
1	DAVDL-ATL-ATS, Structures Tech Area
	Director, U.S. Army R&T Laboratories (AVRADCOM), NASA-Lewis Research Center, Cleveland, OH 44135
1	ATTN: Propulsion Lab
	Director, U.S. Army R&T Laboratories (AVRADCOM), NASA-Langley Research Center, Hampton, VA 23655
1	ATTN: John Shipley, MS266
1	G. L. Roderick, MS266
	Commander, U.S. Army Electronics Research and Development Command, Fort Monmouth, NJ 07703
1	ATTN: DELSD-E, Mr. Stan Alster
1	DELSD-L
	Commander, U.S. Army Scientific and Technical Information Team, 6000 Frankfurt/Main, I. G. Hochhaus, Room 750, West Germany (APO 09710, NY)
1	ATTN: Mr. Charles D. Roach
	Commander, U.S. Army Missile Command, Redstone Arsenal, AL 35809
1	ATTN: DRSMI-TB, Redstone Scientific Information Center
1	Directorate of R&D
1	DRSMI-RLM
1	DRSMI-RLA, Dr. James J. Richardson
1	J. Wright, Jr., Propulsion Director
	Commander, U.S. Army Mobility Equipment Research and Development Command, Fort Belvoir, VA 22060
1	ATTN: DRDME-D
1	DRDME-M
1	DRDME-MD
1	DRDME-V
	Director, U.S. Army R&T Laboratories (AVRADCOM), Moffet Field, CA 94035
1	ATTN: R. L. Foye, MS 207-5
	Commander, U.S. Armament Research and Development Command, Dover, NJ 07801
1	ATTN: Mr. Harry E. Pebly, Jr., PLASTEC, Director
1	Mr. A. Slobodinski
	Commander, U.S. Army Aviation Research and Development Command, 4300 Goodfellow Blvd., St. Louis, MO 63120
1	ATTN: DRDAV-NS, Harold Law
	Director, U.S. Army Ballistic Research Laboratory, Aberdeen Proving Ground, MD 21005
1	ATTN: DRDAR-TSB-S (STINFO)
	U.S. Army Cold Regions Research and Engineering Laboratories Lyme Road, Hanover, NH 03755
1	ATTN: Mr. Ronald Liston
	Commander, U.S. Army Tank-Automotive Command, Warren, MI 48090
1	ATTN: DRSTA-RCKM, Mr. Jim Chevalier
	Watervliet Arsenal, Benet Weapons Laboratory, Watervliet, NY 12189
1	ATTN: G. D'Andrea
1	T. Davidson
1	D. P. Kendall
	Commander, U.S. Military Academy, West Point, NY 10996
1	ATTN: LTC P. D. Heimdaal, Dept. of Mechanics
	Chief, Bureau of Ships, Department of the Navy, Washington, DC 20315
1	ATTN: Code 341
	Chief of Naval Research, Arlington VA 22217
1	ATTN: Code 471
	Director, Structural Mechanics Research, Office of Naval Research, 800 North Quincy Street, Arlington, VA 22203
1	ATTN: Dr. N. Perrone
	David Taylor Naval Ship Research and Development Laboratory, Annapolis, MD 21402
1	ATTN: Dr. H. P. Chu
	Naval Air Systems Command, Washington, DC 20361
1	ATTN: AIR-950D
1	AIR-5163
1	PMA-257
	Naval Air Development Center, Warminster, PA 18974
1	ATTN: Code 6043, Mr. A. Manno
1	Code 6043, Mr. T. Hess
1	Code 6043, Mr. L. Gause
	Naval Sea Systems Command, Washington, DC 20362
1	ATTN: Code 035, Dr. H. Vanderveldt
	Office of Naval Technology, 800 N. Quincy Street, Arlington, VA 22203
1	ATTN: Mr. J. J. Kelly - Code MAT 0715
	Naval Facilities Engineering Command, 200 Stovall Street, Alexandria, VA 22232
1	ATTN: Mr. Robert Peloquin - Code 0320

No. of Copies	To
	Naval Surface Weapons Center, White Oak, Silver Spring, MD 20910
1	ATTN: Steven G. Fishman - Code R32
1	John V. Foltz - Code R32
1	Mr. J. Agul
	Naval Weapons Center, China Lake, CA 93555
1	ATTN: K. Bailey - Code 3383
	Naval Ship R&D Center, Bethesda, MD 20034
1	ATTN: Code 173.2, Mr. Couch
1	Code 2870, Mr. Edelstein
	Naval Research Laboratory, Washington, DC 20375
1	ATTN: Dr. I. Wolock, Code 6307
	Headquarters, U.S. Air Force/RDPI, The Pentagon, Washington, DC 20330
1	ATTN: Major Donald Sponberg
	Headquarters, Aeronautical Systems Division, 4950 TEST W/TZHM (DH 2-5 Mgr), Wright-Patterson Air Force Base, OH 45433
1	ATTN: AFML-MAT8, Mr. George Glenn
	Commander, U.S. Air Force Wright Aeronautical Laboratories, Wright-Patterson Air Force Base, OH 45433
1	ATTN: AFWAL/MLB, F. D. Cherry
1	AFWAL/MLBM, Marvin Knight
1	AFWAL/MLBM, Dr. S. W. Tsai
1	AFWAL/MLBM, J. Whitney
1	AFWAL/FIBCA, C. Wallace
1	AFWAL/FIBE, G. Sendeckyj
1	ASO/ENE, Dr. J. Halpin
	Air Force Office of Scientific Research, Bldg. 410, Bolling AFB, Washington, DC 20332
1	ATTN: LTC J. Morgan
	National Aeronautics and Space Administration, Washington, DC 20546
1	ATTN: AFSS-AD, Office of Scientific and Technical Information
1	Mr. B. G. Achhammer
	NASA-Lewis Research Center, 21000 Brookpark Road, Cleveland, OH 44135
1	ATTN: C. C. Chamis, MS 49-6
1	J. E. Srawley
	NASA-Langley Research Center, Hampton, VA 23665
1	ATTN: J. G. Williams, MS 190
1	J. H. Starnes, MS 190
1	M. F. Card, MS 230
1	R. A. Pride, MS 231
1	C. F. Vosteen, MS 244
1	H. Bohon, MS 158
	National Aeronautics and Space Administration, Marshall Space Flight Center, Huntsville, AL 35812
1	ATTN: R. J. Schwinghammer, EM01, Dir, M&P Lab
1	Mr. W. A. Wilson, EH41, Bldg. 4612
	Federal Aviation Administration, 800 Independence Avenue, Washington, DC 20591
1	ATTN: J. Soderquist, AWS-103
	Brown University, Providence, RI 02912
1	ATTN: Prof. J. R. Rice
	California Institute of Technology, Pasadena, CA 91125
1	ATTN: W. G. Knauss
	Carnegie-Mellon University, Department of Mechanical Engineering, Schenley Park, Pittsburgh, PA 15213
1	ATTN: Dr. J. L. Swedlow
	Carnegie-Mellon University, Mechanical Engineering Department, Scaife Hall, Pittsburgh, PA 15213
1	ATTN: Kai J. Baumann
	Drexel University, Dept. of Mechanical Engineering, Philadelphia, PA 19106
1	ATTN: J. Awerbach
	George Washington University, School of Engineering and Applied Sci., Washington, DC 20052
1	ATTN: Dr. M. Liebowitz
1	E. Altus

No. of Copies	To
	Georgia Institute of Technology, School of Aerospace Engineering, Atlanta, GA 30332
1	ATTN: Lawrence W. Rehfield
	Lehigh University, Bethlehem, PA 18015
1	ATTN: Prof. G. C. Sih
1	Prof. F. Erdogan
	Massachusetts Institute of Technology, Cambridge, MA 02139
1	ATTN: John Dugundji
1	J. W. Mar
1	J. Mandel
1	F. J. McGarry
	Ohio State University, Dept. of Mechanical Engineering, Columbus, OH 43210
1	ATTN: L. S. Han
	Purdue University, W. Lafayette, IN 47907
1	ATTN: C. T. Sun, School of Aero & Astro
	Renselaer Polytechnic Institute, Mechanical Engineering Dept., Troy, NY 12180
1	ATTN: Prof N. Hoff
	State University of New York at Stony Brook, Stony Brook, NY 11790
1	ATTN: Prof. Fu-Pen Chiang, Department of Mechanics
	Texas A&M University, Civil Engineering Dept., Mechanics and Materials Center, College Station, TX 77843
1	*ATTN: R. A. Schapery*
	University of Dayton Research Institute, Dayton, OH 45469
1	ATTN: R. L. Conner
1	J. D. Camping
1	G. J. Roth
1	B. S. West
	University of Delaware, Newark, DE 19711
1	ATTN: J. Vinson, Dept. of Mechanical and Aero Engineering
1	R. B. Pipes, Center for Composite Materials
	University of Illinois, Champaign, IL 61820
1	*ATTN: Prof. D. Drucker, Dean of School of Engineering*
	University of Maryland, College Park, MD 20742
1	ATTN: Dr. George R. Irwin, Department of Mechanical Engineering
	University of Michigan, Mechanical Engineering Department, Ann Arbor, MI 48104
1	ATTN: George Springer
	University of Toronto, Institute for Aerospace Studies, 4925 Dufferin Street, Downsview, Ontario, Canada M3H5T6
1	ATTN: Graham Elliot
1	J. S. Hansen
	University of Utah, Salt Lake City, UT 84112
1	ATTN: Prof. J. Dvorak, Civil Engineering Department
	Virginia Polytechnic Institute, Dept. of Engineering Mechanics, Blacksburg, VA 24060
1	ATTN: C. T. Herakovich
1	*E. Reifsnyder*
1	W. Stinchcomb
	Washington University, Dept. of Mechanical Engineering, Campus Box 1087, St. Louis, MO 63130
1	ATTN: H. Tom Hahn
	West Virginia University, Dept. of Mechanical Engineering, Morgantown, WV 26506
1	ATTN: Nicholas J. Salamon
	Wright State University, Dept. of Mathematics, Dayton, OH 45431
1	ATTN: W. J. Park
	Aeronca, Inc, 1712 Germantown Road, Middletown, OH 45042
1	ATTN: Jerry Tuschner
1	C. L. Amba-Rao
	The Aerospace Corporation, P.O. Box 92957, Los Angeles, CA 90009
1	ATTN: Dr. Ernest G. Kendall

No. of Copies	To
	ARTECH Corporation, 2901 Telestar Court, Falls Church, VA 22042
1	ATTN: Henry Hahn, President
	Arthur D. Little Company, Acorn Park, Cambridge, MA 02140
1	ATTN: Douglas Wilmarth
	Bell Helicopter Textron, P.O. Box 482, Ft. Worth, TX 76101
1	ATTN: Raymond J. Schilts, Jr.
1	David L. Williams
	Boeing Aerospace Corporation, P.O. Box 3999, Seattle, WA 98002
1	ATTN: Don Skoumal, MS 8C-43
	Boeing Aircraft Corporation, P.O. Box 3707, Seattle, WA 98124
1	ATTN: Mr. E. House
1	Mr. J. Hoggatt
1	Mr. H. Syder
1	Mr. Ronald W. Johnson
	The Boeing Company, 1308 Dayton Avenue, N.E., Renton, WA 98055
1	ATTN: Robert E. Jones
	The Boeing Company (BMAC), P.O. Box 3999, MS 41-37, Seattle, WA 98124
1	ATTN: E. T. Bannink, Jr.
	The Boeing Vertol Company, P.O. Box 16858, Philadelphia, PA 19142
1	ATTN: Mr. Robert L. Pinckney, Mail Stop P62-06
1	Mr. E. C. Durchlaub
1	Mr. D. Hoffstedt
	Charles Stark Draper Laboratories, 555 Technology Square, Mail Station 27, Cambridge, MA 02139
1	ATTN: Mr. Jacob Gubboy
	CIBA Geigy Corporation, 10910 Talbert Avenue, Fountain Valley, CA 92700
1	ATTN: Dr. K. Berg
	Dow Corning Corporation, P.O. Box 1767, Midland, MI 48640
1	ATTN: Ron Raney
	General Dynamics, Convair Aerospace Division, P.O. Box 748, Ft. Worth, TX 76101
1	ATTN: Dr. R. Wilkins
1	Dr. W. D. Buntin
	General Dynamics, Fort Worth Division, Ft. Worth, TX 76101
1	ATTN: James Eisenman, P.O. Box 748, MF 2886
1	F. H. Chang, P.O. Box 748, MF 5986
	General Electric Company, Schenectady, NY 12010
1	ATTN: Mr. A. J. Brothers, Materials & Processes Laboratory
	General Electric, Space Systems Division, Rm. M4018, P.O. Box 8555, Philadelphia, PA 19101
1	ATTN: Benjamin T. Rodini, Jr.
	Grumman Aerospace Corporation, Bethpage, NY 11716
1	ATTN: James B. Whiteside, MS A08-35
1	S. J. Dastin, MS B10-25
1	R. N. Hadcock, MS C48-05
	Hughes Helicopters, Centinela Avenue & Teale Streets, Culver City, CA 90230
1	ATTN: Donald H. Mancill
1	George Hoffman
	IIT Research Institute, 10 West 35th Street, Division M, Chicago, IL 60616
1	ATTN: Issac Daniels
1	K. E. Hofer
	Kaman Aerospace Corporation, Bloomfield, CT 06002
1	ATTN: Mr. L. Schuler
	Lear Fan Corporation, Reno, NV 89506
1	ATTN: Mr. R. Abbott
	Lockheed-California Company, Burbank, CA 91503
1	ATTN: Mr. F. English
	Lockheed-California Company, Rye Canyon Research Labs, Burbank, CA 91520
1	ATTN: K. N. Lavraitis, D/74-71, B/204, P2
	Lockheed-Georgia Company, Marietta, GA 30063
1	ATTN: S. Freeman, D/72-53, M S319
	Lockheed Missiles and Space Company, P.O. Box 504, Sunnyvale, CA 94086
1	ATTN: P. J. Moure, Org. 62-60, Bldg. 106

No. of Copies	To
	Lockheed-Palo Alto Research Lab., 3251 Hanova Street, Palo Alto, CA 94306
1	ATTN: D. Flaggs
	Martin Marietta Aerospace, Denver Division, P.O. Box 179, Mail Code 0626, Denver, CO 80201
1	ATTN: Ward D. Rummel
	Material Concepts, Inc., 2747 Harrison Road, Columbus, OH 43204
1	ATTN: Mr. Stan J. Paprocki
	Materials Sciences Corporation, Blue Bell Office Campus, Blue Bell, PA 19422
1	ATTN: N. Dow
1	K. Boesking
1	Dr. B. W. Rosen, Pres.
	McDonnell Douglas, Corp., Douglas Aircraft Co., 3855 Lakewood Blvd., Long Beach, CA 90801
1	ATTN: T. Gresczuk
1	C. Stephens
	McDonnell Douglas Corporation, McDonnell Aircraft Co., P.O. Box 516, St. Louis, MO 63160
1	ATTN: Harold D. Dill
1	Samuel P. Garbo
	Northrup Corporation, 3901 West Broadway, Hawthorne, CA 90250
1	ATTN: G. Grimes
1	N. Bhatia
1	R. L. Ramkumar
1	R. S. Whitehead
	Price Brothers Company, P.O. Box 825, Dayton, OH 45401
1	ATTN: O. L. Schlecel
	Rockwell International, Downey, CA 90241
1	ATTN: Mr. W. H. Morita
	Rockwell International, P.O. Box 51308, Tulsa, OK 74151
1	ATTN: F. S. Spears
	Rockwell International, P.O. Box 92098, Los Angeles, CA 90009
1	ATTN: Donald Konishi
	Rohr Industries, P.O. Box 878, Chula Vista, CA 92012
1	ATTN: J. R. Goulding
	Shell Development Company, Weshollow Research Center, P.O. Box 1380, Houston, TX 77001
1	ATTN: King Him LO
	Sikorsky Aircraft, Stratford, CT 06602
1	ATTN: Mr. M. J. Rich
1	Mr. J. D. Ray
1	Mr. V. Chase
	Solar Energy Research Institute, 1536 Cole Boulevard, Golden, CO 80401
1	ATTN: Dr. J. Charles Grosskreutz, Asst. Dir. for Research
1	Southwest Research Institute, 8500 Culebra Road, San Antonio, TX 78284
	Systems Research Laboratories, Inc, 2800 Indian Ripple Road, Dayton, OH 45440
1	ATTN: Y. Bar-Cohen
	TM Development, Inc, J E N Industrial Campus, 2540 Green St., Chester, PA 19013
1	ATTN: Craig D. Thompson
	TRW Systems, One Space Park, Redondo Beach, CA 90278
1	ATTN: Waleed F. Rahhal, R5/B221
	Universal Energy Systems, 3195 Plainfield Road, Dayton, OH 45432
1	ATTN: Sam Soni
	United Technologies Research Center, Mail Stop 24, East Hartford, CT 06108
1	ATTN: Dr. Karl M. Prewo, Principal Scientist
	Vought Corp., Advanced Technology Center, Dallas, TX 75266
1	ATTN: J. Renton
	Westinghouse Research and Development Center, 1310 Beulah Road, Pittsburgh, PA 15235
1	ATTN: Mr. E. T. Wessel
	Director, Army Materials and Mechanics Research Center, Watertown, MA 02172
2	ATTN: DRXMR-PL
3	Authors

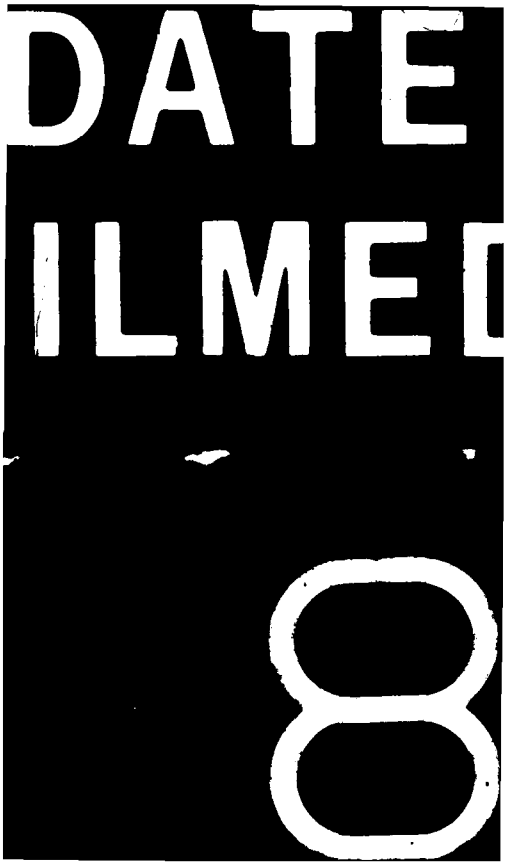
DATE
ILMED
8